Physica Scripta. Vol. T59, 236–243, 1995

Trapped Metal Cluster Ions

L. Schweikhard[1], St. Becker[1]*, K. Dasgupta[2], G. Dietrich[3], H.-J. Kluge[1]†, D. Kreisle[4], S. Krückeberg[1], S. Kuznetsov[5], M. Lindinger[1], K. Lützenkirchen[2], B. Obst[1], C. Walther[1], H. Weidele[4] and J. Ziegler[1]

[1] Institut für Physik, Johannes Gutenberg-Universität, D-55099 Mainz, Germany
[2] Bhabha Atomic Research Center, Bombay 400085, India
[3] Institut für Kernchemie, Johannes Gutenberg-Universität, D-55099 Mainz, Germany
[4] Fakultät für Physik, Universität Konstanz, D-78434 Konstanz, Germany
[5] Department of Chemistry, Moscow State University, 119899 Moscow, Russia

Received August 19, 1994; accepted in revised form March 9, 1995

Abstract

An overview is given of experiments with stored metal cluster ions in a Penning trap system. The setup allows axial injection of clusters produced in an external source and a time-of-flight mass analysis of the reaction products after axial ejection. The system's options include the selection of stored ions, the manipulation of their orbits, addition of reactant and buffer gases and axial optical access for laser spectroscopic studies. As described by various examples, investigations have been made with respect to the development of trapping techniques and the characterization of metal clusters in terms of their physical and chemical properties.

1. Introduction

Metal clusters have gained considerable interest since the observation of "magic numbers" in abundance spectra [1] which was explained in terms of shell models of the delocalized atomic valence electrons [2, and references therein]. Several experiments have been performed (for an overview see Ref. [3] and the proceedings of recent conferences [4]) mostly dealing with supported clusters (on substrates or embedded in rare gas matrices) or with cluster beams. It has been realized [5, 6, 7], however, that the storage of clusters in ion trapping devices has several advantages: The clusters are "free", e.g. they do not interact with substrate or matrix atoms; the cluster sizes of interest may be selected by ejection of unwanted species; the clusters may be prepared by various interactions, e.g. cooling by a buffer gas; several sequential reaction/selection events are possible; all ionic reaction products stay in the trap and may be further analyzed. Cluster ions may be "grown" inside a trap and the production of H_n^+ clusters from H_3^+ condensation seeds in a cold hydrogen environment has been studied in detail by use of a 22-pole rf trap [8]. On the other hand the use of external cluster sources (i.e. the creation of cluster ions outside of and transfer into the trap) allows a broad range of production methods.

In this paper we describe experiments performed with a Penning trap system including an external cluster ion source and a time-of-flight mass spectrometer for product analysis. The next sections give an overview of the experimental setup and procedures. They are followed by a description of the system's performance including Penning trap developments. Finally examples of investigations on stored metal clusters are given: collision induced dissociation, chemical reactions, photofragmentation and electron detachment studies.

2. Experimental setup

The experimental setup comprises several components each optimized for its specific function [9]. It will be described in detail elsewhere. In the following we give a summary of the functions and properties of the main constituents (see also Fig. 1). Further details of importance are discussed in the section describing various experiments.

2.1. *Cluster ion source*

Clusters are produced by focusing the frequency-doubled light of a Q-switched Nd : YAG laser onto a metal wire and simultaneous injection of a pulse of helium into the vaporization chamber [10]. The vaporized material (neutral or ionized) forms clusters in the helium atmosphere. They are subsequently cooled during an adiabatic expansion through a nozzle into the vacuum. No postionization is applied. Instead, primary cluster ions (both positive and negative) are extracted from the source for the experiments described below. Singly-charged gold clusters of up to 145 atoms, i.e. at $m = 28\,560$ u, have been produced in this external source, transferred and stored in the trap [11].

2.2. *Transfer section*

The cluster ions are guided from the external source towards the Penning trap by several arrays of electrostatic lenses and deflectors. The ion-transfer section includes several skimmers and diaphragms for differential pumping to maintain the pressure in the UHV sections (trap and time-of-flight) in the 10^{-8}-mbar range while it may be well above 10^{-3} mbar in the source chamber.

2.3. *Penning trap*

Cluster ion trapping is provided by a Penning trap [12]: a combination of a homogeneous magnetic field of $B = 5$ T and an axial quadrupolar electric field

$$E = \frac{U}{2d^2}(x, y, -2z),$$

produced by connecting two endcap electrodes and the segments of a ring electrode with suitable electric potentials. The difference of these potentials, U, is typically a few volts, the trap dimension [12] $d^2 = 200\,\mathrm{mm}^2$. The ion motion and

* Present address: iC-Haus, Am Kuemmerling 18, D-55294 Bodenheim, Germany.
† Present address: GSI Darmstadt, Postfach 110 552, D-64220 Darmstadt, Germany.

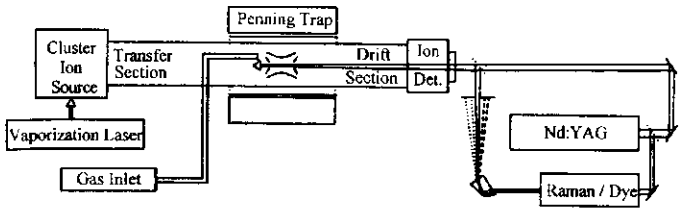

Fig. 1. Overview of the experimental setup including the vacuum system with cluster ion source, transfer section, Penning trap, drift section and ion detector. In addition the gas inlet system and laser systems for cluster production and photoexperiments on stored cluster ions are indicated.

trapping conditions are described below. The ring electrode has been segmented to allow various manipulations of the ion motion [13]. The mass dependence of the cyclotron frequency (see below) may be used for an analysis of the stored ions by excitation to coherent motions and pickup of the image charges induced in the trap electrodes (FT-ICR MS: Fourier Transform – Ion Cyclotron Resonance Mass Spectrometry [14]). While the setup has been used for FT-ICR developments earlier [15, 16] these will not be discussed in this contribution. Instead, time-of-flight detection and analysis has been used for the present experiments.

2.4. *TOF section*

The Penning trap serves as the first section of a two-stage time-of-flight (TOF) mass spectrometer [17]. By use of a microchannel plate (MCP) detector at the end of a 2-m drift tube single ion counting at low noise rate is achieved. To allow optical access to the trap along the axis, and also to increase the sensitivity, the cluster ions may be directed onto a conversion electrode [18]. The secondary electrons (or secondary ions when cluster anions are investigated) are detected on a MCP arrangement that is mounted off the z-axis.

2.5. *Gas inlet system*

Three storage vessels allow the preparation of gas mixtures. The gas is led to the trap by two tubes (Fig. 1), either continuously or in a pulsed mode. The latter is achieved by gating a piezo valve next to the Penning trap [19].

2.6. *Laser systems*

The second, third and fourth harmonic of a Nd : YAG laser and the corresponding Raman-shifted light from a hydrogen cell are available for experiments on cluster-photon interactions. In addition, the Nd : YAG laser is used to pump a dye laser system. The resulting light may be frequency doubled before it is sent axially into the Penning trap. The laser spot at the position of the trap is monitored on line by deflection of a small percentage of the beam onto a CCD camera. Furthermore, a CO_2-laser may be used for infrared studies.

2.7. *Experimental control and data evaluation*

The experimental sequences are produced by home-built CAMAC memory modules. These are programmed by PC and VME-bus routines. Single-ion-counting time-of-flight spectra are taken by sending the MCP pulses to a discriminator and its output pulses to a transient recorder. The data are evaluated on-line by the PC and transferred to the computer clusters of the institutes of physics and nuclear chemistry for storage and further evaluation.

3. Experimental sequence

A typical experimental sequence consists of the following events: After (i) their production in the external source the cluster ions are (ii) transferred to the Penning trap. Both the temporal width of the cluster bunch from the source and the transfer duration are of the order of a millisecond. The potential of the entrance endcap is pulsed down and (iii) a selected distribution of cluster ions is captured in flight [20]. Then, (iv) the axial ion motion is cooled (for a few tens of milliseconds) via a buffer gas from the pulsed piezo valve inlet. This section of events may be repeated several times for cluster accumulation in the trap [19]. Afterwards (within a few milliseconds) the cluster species of interest is (v) selected by radial ejection of all unwanted ions. The remaining clusters are (vi) brought into interaction with their reaction partners (neutral atoms or molecules, electrons, ions, photons) and are (vii) given a variable time for delayed reactions. The selection/reaction part of the sequence may again be repeated, with variations of the selection range and reaction period from cycle to cycle, constituting several combined mass spectrometry (MS) experiments. An extreme example of such an experiment has been performed by Irion *et al.* who demonstated in an MS^5 FT-ICR investigation that benzene can be "grown" from C_2H_2 on Fe_4^+ [21]. Finally the ions are (viii) ejected axially from the trap for a time-of-flight mass analysis of the reaction products. Depending on the clusters' mass and charge the time of flight may last several hundreds of microseconds. However, a metastable fragmentation (into ionic pieces) during the drift to the ion detector has no influence on the fragment distribution of the observed spectrum which represents the distribution at the time of ejection from the Penning trap. The whole sequence is repeated from a few up to several thousand times to increase the statistical significance of the data.

4. System performance and ICR trap developments

4.1. *Cluster source and transfer*

Due to collisions with helium atoms during the expansion into the vacuum the cluster ions are cooled and accelerated towards the Penning trap. To support their extraction from the source a potential difference of 100 volts is applied between the source body and the transfer section. Therefore the singly charged clusters gain an additional kinetic energy of 100 eV. When they arrive at the trap they are slowed down by application of an offset potential to the Penning trap electrodes. The appropriate offset is a function of cluster size, n. In Fig. 2 the number of trapped gold cluster ions, Au_n^+, is given as a function of the offset potential of the Penning trap. It shows the distribution of axial kinetic energies for each size, n. The values of the mean energy as a function of cluster size n can be fitted to a straight line ($100\,\text{eV} + 1.7\,\text{eV} \times n$).

4.2. *Ion selection*

As described above, the choice of the trap offset potential leads to a preselection of the trapped cluster species. A specific cluster size is selected by the additional use of radial ejection of the unwanted cluster sizes after they have already been captured. As an example, the upper mass spectrum of

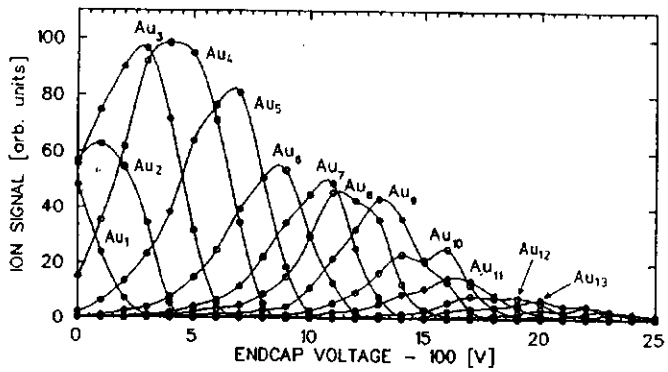

Fig. 2. Intensities of captured gold cluster ions (of size $n = 1$ to 13, as indicated) as a function of the potential offset applied to the Penning trap. For details see text.

Fig. 3 shows the distribution of tungsten cluster anions, W_n^-, with n ranging from 6 to 10, as captured in the Penning trap. For the experiments on size selected clusters, all unwanted masses are ejected by excitation of their cyclotron motion (see below). This procedure increases the cyclotron radius until the unwanted cluster ions hit the ring electrode of the trap. The lower part of Fig. 3 shows the spectrum after all clusters, except for W_8^- are ejected. Note that tungsten has several stable isotopes. Hence, for a given cluster size quite a few isotopic combinations are possible. These different cluster masses are not resolved in the TOF spectrum. However, the radial ejection has enough resolving power to selectively remove unwanted isotopic combinations, if desired. At the same time, cluster-molecule complexes that may be delivered from the source but are not of interest for the current investigation may also be removed by radial ejection.

4.3. *Stability of ion orbits*

The upper part of Fig. 4 shows a typical ion motion. It consists of three independent modes:

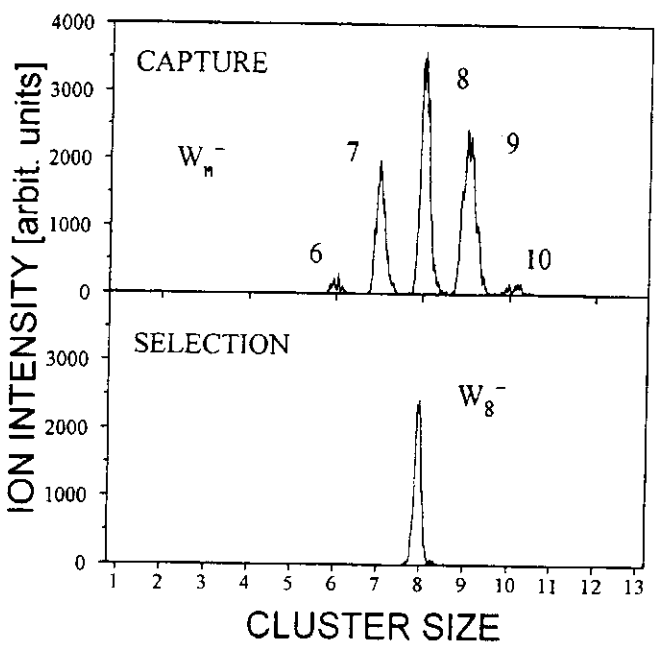

Fig. 3. Mass spectra (sum of 100 transients) from TOF measurements of W_n^- after capture (top) and after additional selection of W_8^- by radial ejection of all other cluster species (bottom). Note that the W_8^--signal intensity is decreased by the selection, since high-mass isotopic combinations and possible W_8^- ions with adsorbed molecules have been ejected as well.

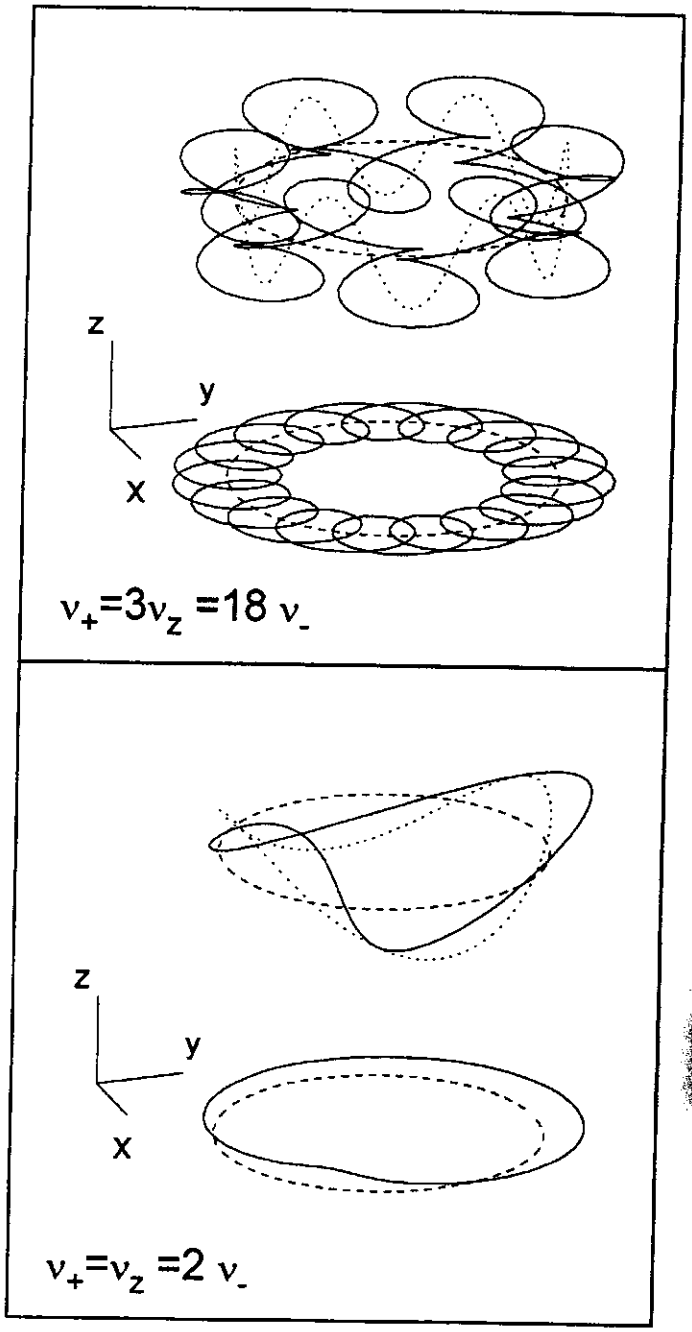

Fig. 4. Ion trajectory in a Penning trap. Dashed line: Magnetron motion only; dotted line: combined magnetron and trapping motion; solid line: full ion motion, i.e. combined magnetron, cyclotron, and trapping motion. Top: for $\nu_+ = 3\nu_z = 18\nu_-$. Bottom: for $\nu_+ = \nu_z = 2\nu_-$ (corresponding to $\pi_{trap} = 8/9$).

(i) The circular cyclotron motion (of angular frequency ω_+),
(ii) the circular magnetron motion (ω_-), and
(iii) the harmonic trapping (axial, or z-) oscillation (ω_z).
The frequencies are defined by the trap parameters (B, U, d) and the ions mass-over-charge ratio (m/q):

$$\omega_z = \sqrt{\frac{qU}{md^2}}, \quad \omega_\pm = \frac{\omega_c}{2} \pm \sqrt{\frac{\omega_c^2}{4} - \frac{\omega_z^2}{2}},$$

where $\omega_c = qB/m$ is the cyclotron frequency in the absence of the electric trapping potential. The ion orbits are only stable as long as the argument in the square root of $\omega_\pm$ is positive. For a given set of trap parameters and ion charge, this sets a limit for the highest ion mass (often called "critical mass"), i.e. largest cluster size, that may be trapped. We

have tested the trapping performance for singly charged ions up to mass $m = 28\,560$ amu (Au_{145}^-). During these investigations another kind of instability has been found [11]. It occurs at $\pi_{trap} = 8/9$, where the trapping parameter π_{trap} has been defined as $\pi_{trap} = 2\omega_z^2/\omega_c^2$. ($\pi_{trap} = 1$ corresponds to the critical mass.) Another way to describe the condition for the new instability is in terms of the relation of the frequencies of ion motions: $\omega_+ = \omega_z = 2\omega_-$. The bottom part of Fig. 4 shows the ion orbit for a particular set of amplitudes and phases of this closed ion trajectory. Turn after turn the ions see the same perturbations of the trapping field. In analogy to the stopping bands of particle storage rings the ions are eventually lost from the trap. While this instability is interesting in itself it poses no serious problem to the cluster investigations, since it reduces the unperturbed mass range by a factor of 8/9, only.

4.4. *Centering of trapped cluster ions*

After the ions are captured their motion may be slowed down by application of buffer gas cooling. Collisions with buffer gas atoms (argon) lead to reduced amplitudes of the cyclotron and trapping motion. The magnetron orbits, however, tend to grow when buffer gas cooling (or any frictional force, in general) is applied. Therefore the magnetron motion is converted into cyclotron motion by radial quadrupolar excitation [22]. This results in an overall axialization and centering of the ion cloud [23–25]: SQUEACE (selective quadrupolar excitation assisted centering [19]). The cluster ion distribution has been determined by photofragmentation of gold cluster ions (see below). While the laser spot is scanned across the trap, the number of fragment ions is determined as a function of the spot position. The cluster cloud can be approximated by a Gaussian distribution with a full width at half maximum of about 1 mm to 3 mm (depending on the particular clusters and trap parameters).

5. Measurements on stored cluster ions

The system has been built for experiments with respect to the properties of metal cluster ions [6]. These investigations include the interaction with neutral atoms, as in collision induced dissociation or reactions with molecules, and the interaction with laser light, as in photofragmentation and photodetachment studies. A few examples are given in the following sections.

5.1. *Collision induced dissociation*

A large variety of possible studies in the field of ion-atom/molecule collisions has been reviewed recently [26]. One of these, collision induced dissociation (CID), is an important mass spectrometric technique for structural analysis. It has been used extensively on trapped ions after Cody *et al.* introduced it to FT-ICR experiments [27]. The ions under investigation are accelerated by excitation of their cyclotron motion and collide with neutral atoms. Thereby kinetic energy is converted into internal energy which eventually results in fragmentations. This method has been employed for the study of small gold clusters, Au_n^+, $n = 2, 3, \ldots, 23$ [28–30]. Neutral atoms and dimer evaporation from the precursor cluster ion has been observed as well as sequential decay processes, e.g. $Au_7^+ \rightarrow Au_5^+ \rightarrow Au_3^+$. The direct decay, $Au_7^+ \rightarrow Au_3^+$, can be excluded by a double-resonance technique: While Au_7^+ is accelerated and given time to collide and fragment, Au_5^+ is constantly ejected from the trap by excitation of its cyclotron motion (as for the ejection of unwanted ion species, see above). For this experimental sequence, no Au_3^+ fragment is observed, confirming that Au_7^+ decays via Au_5^+. Another important value to be determined is the threshold energy for fragmentation. It shows an odd-even alternation that can be understood within the framework of the shell models mentioned in the introduction [2].

While these measurements have been performed "conventionally", i.e. with an excitation of the cyclotron motion, we have shown recently, that CID via the trapping motion ("axial CID") is possible as well. This is demonstrated in Fig. 5: TOF spectra of axial CID of Au_5^+: The upper spectrum is that of a reference measurement, where no excitation of the trapping motion has been applied. The lower spectrum shows the fragment ion pattern after axial CID. These spectra have been recorded "quasi simultaneously": They both are the sum of 100 transients, where reference and CID cycles have been alternated. Axial CID may be of special interest for high mass ions (already Au_5^+ has a mass of 985 u). In this case the energy of the trapping motion is comparable to – and for an elongated trap configuration may well exceed – the maximum kinetic energy of the cyclotron motion. Furthermore, with the axial CID technique the collisions occur in the trap center which is best suited for subsequent detection of the product ions. This is opposed to the conventional (cyclotron) CID, where the collisions take place far from the trap axis which complicates the detection

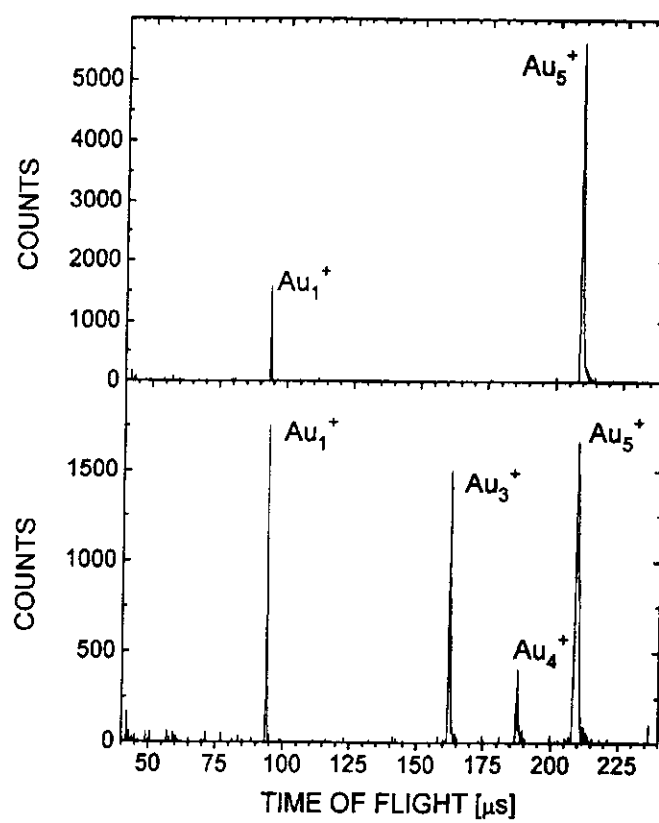

Fig. 5. TOF spectra demonstrating axial CID of Au_5^+: Top: ion distribution after capture and selection of Au_5^+ (trap potential $U = 29$ V). Bottom: in addition, axial CID is applied (80 ms at $n = 19.2$ kHz). Note that the scale of the ordinate has been changed. For better comparison, the atomic gold ion, Au^+, has not been ejected.

of the fragments. More details on axial CID will published elsewhere.

5.2. *Chemical reactions*

Small gold cluster ions have also been probed with respect to their chemical behavior towards N_2O [31]. In this contribution, however, we want to turn to a different element and report preliminary results from vanadium clusters exposed to hydrogen. The three spectra of Fig. 6 show the intensity of bare V_n^+, with $n = 5$ to 11, after these clusters have been exposed to hydrogen at a pressure of 8×10^{-6} mbar. Note that the spectra shown are difference spectra from two types of experimental sequences. Several transients of each type have been taken alternately. In the type 1 sequences no radial ejection is applied and all clusters are detected. In the type 2 sequences the bare vanadium clusters are radially ejected just before mass analysis/detection. While the resolving power of the TOF spectrometer is not sufficient to directly determine the intensities of the various $V_nH_m^+$ clusters this may be achieved by the double mass spectrometry experiment involving the high-resolution mass-selective radial ejection plus the low-resolution, but highly-sensitive TOF analysis: The difference spectra of Fig. 6 (spectra of type 1 minus spectra of type 2 sequences) show the bare cluster ions that survived the storage period (60, 160 and 1560 ms) without reaction with H_2. There are two advantages of this method as compared to the complementary technique of ejecting all clusters with adsorbates ($V_nH_m^+$) and leaving the bare clusters only for direct detection:

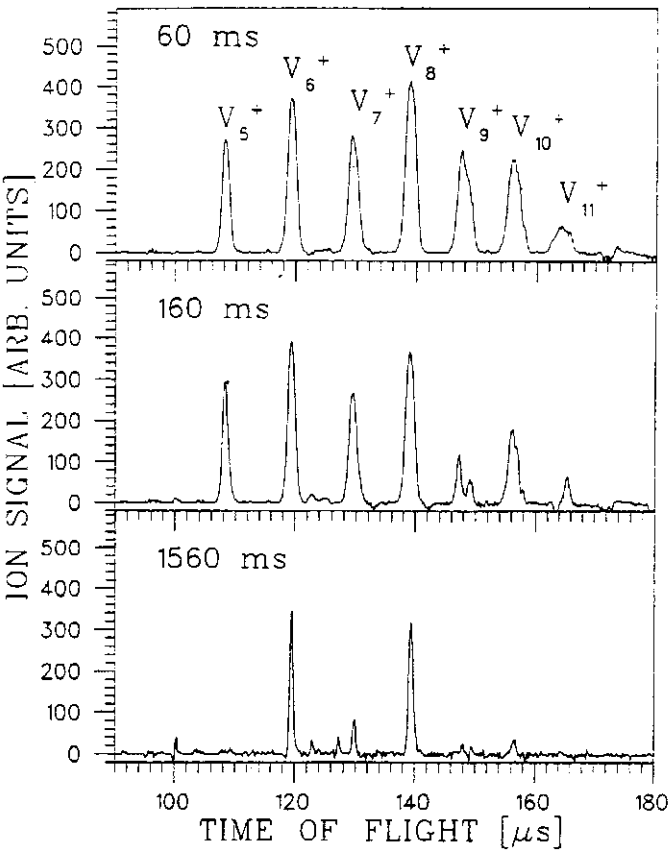

Fig. 6. TOF spectra of surviving bare V_n^+ clusters after 60 ms (top), 160 ms (middle) and 1560 ms (bottom) of exposure to a hydrogen atmosphere of 8×10^{-6} mbar. Each spectrum is calculated as a difference of transients (sums of 2000, 1000 and 750, respectively) as explained in the text. (The resolving power of the TOF spectra increases with storage duration due to the cooling ion motion.)

(i) The number of hydrogen atoms adsorbed may vary over a broad range. For example, for V_{10}^+ up to 12 adsorbed hydrogen atoms have been found. For a direct detection of V_{10}^+ all possible combinations have to be considered.

(ii) By dividing the difference intensities with those from sequences of type 1 the intensities are normalized and fluctuations and drifts, e.g. of the production rate of the cluster source, cancel.

From spectra like the ones of Fig. 6 reaction rate constants may be determined. (For the cluster size range of Fig. 6 they range from 10^{-12} to $10^{-10}\,cm^3\,s^{-1}$ and show an odd/even alternation.) Furthermore, the maximum number of hydrogen atoms attached to the cluster ions has been measured. Also, by collision induced dissociation, it may be investigated whether the hydrogen molecules dissociate when they react with the cluster. These data are still being evaluated and will be published elsewhere. Adsorption studies can also play an important role in the elucidation of the cluster structures. For example, Elkind *et al.* have found structural isomers via the deuterium takeup of niobium clusters stored in a trap [32].

5.3. *Photofragmentation*

Recently, we have started laser spectroscopic studies on stored metal cluster ions. These include photofragmentation experiments [33, 34] and the photodetachment of electrons (next section). Several of the techniques already mentioned above are combined for these investigations. Figure 7 demonstrates the experimental sequence. TOF mass spectra of several stages of the sequence are shown. The top spectrum was taken after the capture of the pulse of gold cluster ions, Au_n^+. It shows a distribution similar to the one of W_n^- in Fig. 2. For the second spectrum additional buffer gas cooling/quadrupolar excitation was applied. The centering effect of the latter increases the observed ion intensity at the corresponding mass, in this case Au_9^+. Afterwards, all clusters except the one of interest are ejected and Au_9^+ is selected for photofragmentation. The bottom spectrum shows the resulting cluster distribution, 50 ms after the pulse of the fragmentation laser (in this case a 12-mJ laser pulse at a wavelength of $\lambda = 355$ nm). The intensity of the Au_9^+-signal is reduced significantly (note the change in the y-scale). The pattern of fragment cluster ions is very similar to that of the CID studies (see above). While the fragmentation pattern is interesting in itself, another important experimental result is the cross section of photoabsorption. The laser intensity has been varied in order to distinguish between one- and two-photon fragmentation. The overlap of the cluster distribution and the laser profile are modelled and the absorption cross section σ is determined from the fragment intensity. The measurements have been performed for several wavelengths and the result is shown in Fig. 8. The cross section as a function of photon energy shows one very broad resonance feature centered at about 4 eV with a FWHM of about 0.5 eV. It may be interpreted as a collective oscillation of the valence electrons with respect to the ionic core of the cluster, similar to the protons' and neutrons' collective oscillation in the giant dipole resonance of atomic nuclei.

Note that while in this description the absorption of the photon leads to a collective electron motion, the absorption is detected via the fragmentation of the cluster, i.e. the

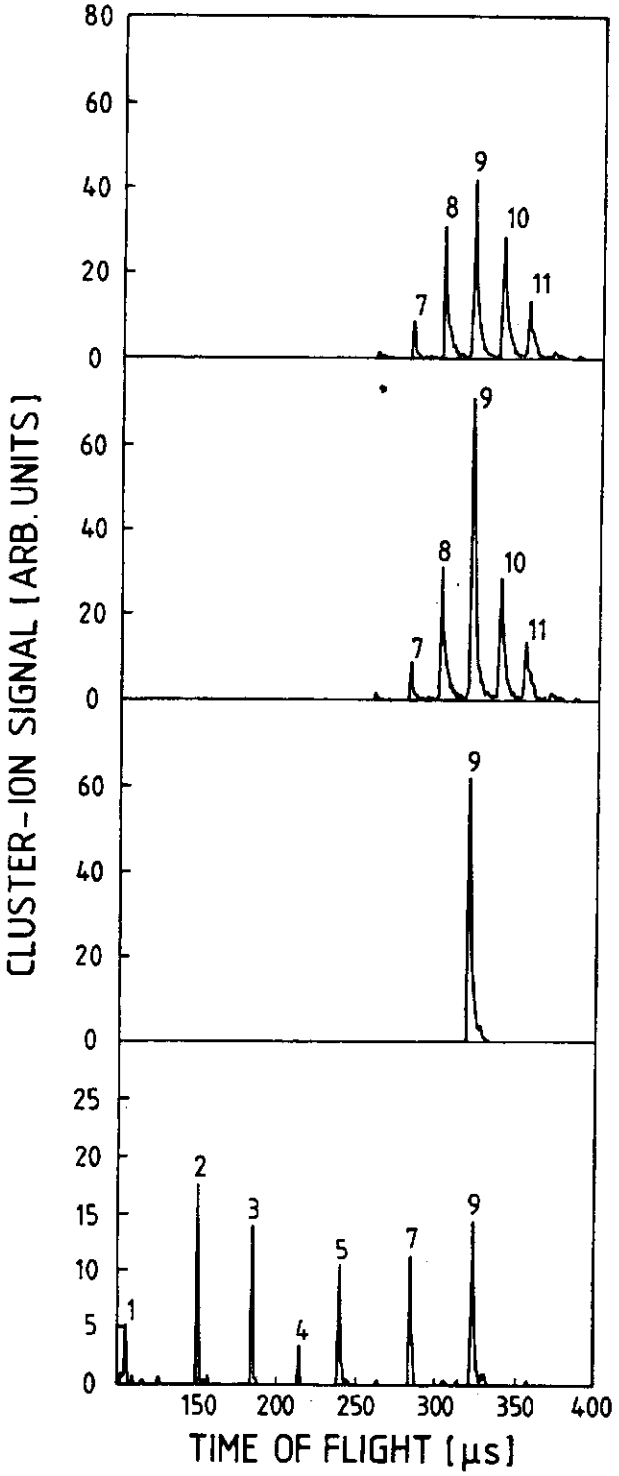

Fig. 7. TOF spectra demonstrating the sequence of events for the photofragmentation of mass selected, centered gold cluster ions, Au_9^+. From top to bottom: Capture of gold cluster ions, size $n = 7$ to 11, as indicated; application of SQUEACE for centering; selection of Au_9^+ by radial ejection of all other cluster species; the distribution of precursor and fragment ions after the application of the fragmentation laser.

energy has been distributed to various degrees of freedom and has finally concentrated in one vibrational mode. Hence, it may be expected that this internal transfer of energy takes some time, i.e. that metastable decays can be observed. Therefore, we have studied the temporal development of the fragmentation pattern. Figure 9 shows the intensities of the fragment cluster ions at several times after the silver (note the switch of element) cluster Ag_{21}^+ has been excited. While the intensities of the precursor and all clusters with $n \leqslant 18$ stay constant, the Ag_{20}^+ ions decay to Ag_{19}^+ in the time range of about 2 ms. The fragmentation behavior may be explained qualitatively by considering the number of photons absorbed by the selected Ag_{21}^+ cluster. Some will not absorb any photon and do not fragment. Others absorb more than one photon and therefore decay fast to small cluster sizes $n \leqslant 18$. Finally, the precursors Ag_{21}^+ that absorb just one photon decay to the next smaller cluster size "spontaneously", i.e. in a period short compared to the duration of extraction from the Penning trap (about 20 μs). These primary fragment products, Ag_{20}^+, continue to decay to Ag_{19}^+, as shown in Fig. 9. The time constant of this decay is a function of the photon energy. Analogous studies on Au_{21}^+ yield similar time constants, however, not for a sequential decay of the primary fragment clusters, but, in contrast, for

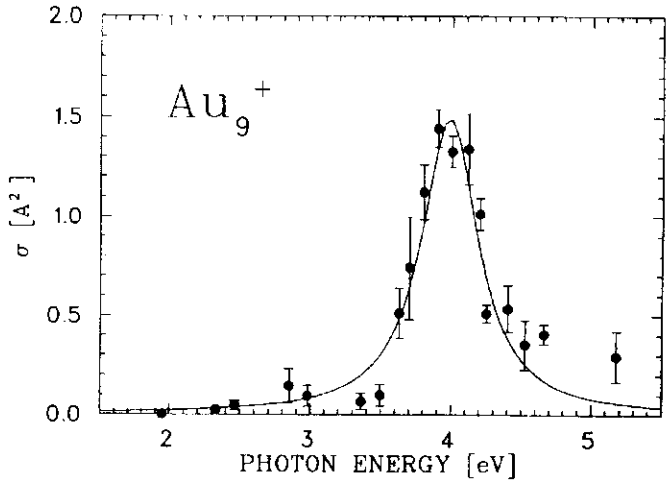

Fig. 8. Photoabsorption cross section of Au_9^+ as a function of photon energy.

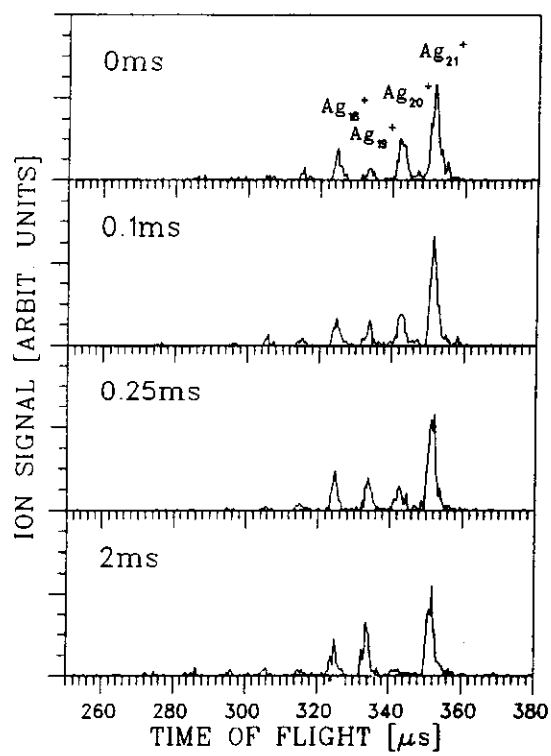

Fig. 9. TOF spectra (sums of 100 transients) after selection of Ag_{21}^+ and application of a laser pulse ($\lambda = 326$ nm, pulse energy 0.35 mJ, laser spot diameter about 5 mm), with delay periods between the photoexcitation and the mass analysis as indicated.

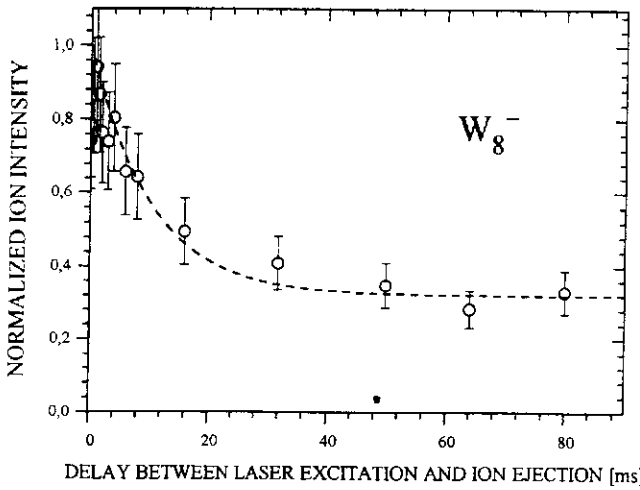

Fig. 10. Normalized ion intensity of W_8^- as a function of the delay between photoexcitation (at $\lambda = 532$ nm, pulse energy 3 mJ, laser spot diameter about 2 mm) and ejection from the trap.

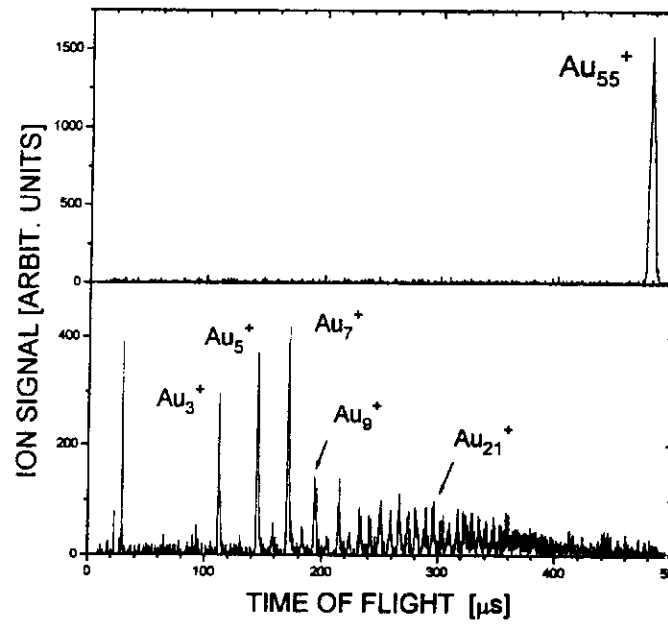

Fig. 11. TOF spectra (sums of 500 transients) of "extended" photofragmentation of Au_{55}^+. Top: selection of Au_{55}^+, no application of fragmentation laser. Bottom: after application of fragmentation pulses (14 × 15 mJ).

the decay of the precursor itself. The different behavior of silver and gold clusters corresponds to their respective atomic binding energies.

5.4. *Delayed electron emission*

As a last example similar laser experiments are presented which have been performed with tungsten cluster anions. In this case the atomic binding energy exceeds the electron affinity. Therefore, it is energetically more favorable for the cluster to emit an electron than to fragment. Indeed, no fragments are observed, while the intensity of the precursor cluster ions decreases as a function of time. This temporal behavior is plotted in Fig. 10 for the case of W_8^-. An exponential function has been fitted to the data (with an additional constant term taking care of the clusters that have not absorbed enough photons for electron detachment). The decay constant is about 10 ms. The delayed electron detachment may be interpreted as a thermionic emission, similar to that known from heated surfaces. The experiments extend to delay times (between laser pulse and mass analysis) of up to half a second. Ion trapping devices are best suited for these kinds of investigations. More details on the tungsten experiments are found in a preliminary publication [35]. Complementary photodetachment experiments where the neutral clusters are detected are possible in heavy-ion storage rings; see for example the investigations on negative fullerene ions performed by the Aarhus group [36].

6. Conclusion and outlook

We have described several experiments performed with a Penning trap system supplemented by an external cluster-ion source and a time-of-flight section. The investigations include developments and studies of the Penning trap itself, like the technique of ion-bunch accumulation and the investigation of the stability of high-mass ion trajectories. The main emphasis, however, is on the study of the properties of metal clusters. Their interaction with neutral noble gas atoms, molecules, and photons has been investigated. The observed reaction channels include the (delayed) fragmentation of the cluster, the adsorption of molecules, and delayed electron emission. We plan to extend these studies to other elements and bigger clusters. Figure 11 shows a preliminary result of the photofragmentation of Au_{55}^+. Repeated laser pulses have been used to break the precursor (Au_{55}^+, top of figure) into pieces. This is a complementary way of producing small clusters as compared to the "synthetic" approach in the cluster ion source. Nevertheless, the resulting cluster spectrum reflects a well-known feature: Due to their higher stability the odd-size clusters are by far more abundant than the even-size clusters. Similar experiments are currently under way with the fragmentation laser replaced by an electron gun. In this case not only fragmentation is observed, but in addition higher charge states show up. Future experiments will also include collisions of cluster ions with each other. Note that all products of primary reactions (as e.g. the highly-charged cluster ions resulting from electron impact ionization) may again be selected and investigated by subsequent interactions.

Acknowledgements

The experiments have been supported by the Deutsche Forschungsgemeinschaft, the Materialwissenschaftliches Forschungszentrum of the Johannes Gutenberg-Universität of Mainz and the European Community. K. Dasgupta thanks for the support under the Indo-German Collaboration between the Bhabha Atomic Research Center, Bombay and the Internationales Büro, KFA Jülich, Germany. S. Kuznetsov acknowledges support from the Deutscher Akademischer Austauschdienst, DAAD, and the Forschungszentrum Karlsruhe.

References

1. Knight, W. D. *et al.*, Phys. Rev. Lett. **52**, 2141 (1984).
2. Brack, M., Rev. Mod. Phys. **65**, 677 (1993).
3. De Heer, W. A., Rev. Mod. Phys. **65**, 611 (1993).
4. Z. Phys. **D19** and **D20** (1991); Z. Phys. **D26** (1993).
5. Alford, J. M., Williams, P. E., Trevor, D. J. and Smalley, R. E., Int. J. Mass Spectrom. Ion Processes **72**, 33 (1986).
6. Kluge, H.-J., Schnatz, H. and Schweikhard, L., Z. Phys. **D3**, 189 (1986).
7. Irion, M. P., Selinger, A. and Wendel, R., Int. J. Mass Spectrom. Ion Processes **96**, 27 (1990).

8. Gerlich, D., Physica Scripta **T59**, 256 (1995).
9. Moore, R. B. *et al.*, Physica Scripta **T59**, 93 (1995).
10. Weidele, H., Frenzel, U., Leisner, T. and Kreisle, D., Z. Phys. **D20**, 425 (1991).
11. Schweikhard, L., Ziegler, J., Bopp, H. and Lützenkirchen, K., Int. J. Mass Spectrom. Ion Processes **141**, 77 (1995).
12. Brown, L. S. and Gabrielse, G., Rev. Mod. Phys. **58**, 233 (1986).
13. Schweikhard, L. and Marshall, A. G., J. Am. Soc. Mass. Spectrom. **4**, 433 (1993).
14. Marshall, A. G. and Schweikhard, L., Int. J. Mass Spectrom. Ion Processes **118/119**, 37 (1992).
15. Schweikhard, L., Lindinger, M. and Kluge, H.-J., Int. J. Mass Spectrom. Ion Processes **98**, 25 (1990).
16. Schweikhard, L., Lindinger, M. and Kluge, H.-J., Rev. Sci. Instrum. **61**, 1055 (1990).
17. Wiley, W. C. and McLaren, I. H., Rev. Sci. Instrum. **26**, 1150 (1995).
18. Daly, N. R., Rev. Sci. Instrum. **31**, 264 (1960).
19. Hasse, H.-U. *et al.*, Int. J. Mass Spectrom. Ion Processes **132**, 181 (1994).
20. Schnatz, H. *et al.*, The ISOLDE Collaboration, Nucl. Instr. Meth. **A251**, 17 (1986).
21. Schnabel, P., Weil, K. G. and Irion, M. P., Angew. Chem. **104**, 633 (1992).
22. Bollen, G., Moore, R. B., Savard, G. and Stolzenberg, H., J. Appl. Phys. **68**, 4355 (1990).
23. Savard, G. *et al.*, Phys. Lett. **A158**, 247 (1991).
24. Schweikhard, L., Guan, S. and Marshall, A. G., Int. J. Mass Spectrom. Ion Processes **120**, 71 (1992).
25. Marshall, A. G. and Guan, S., Physica Scripta **T59**, 155 (1995).
26. Dunn, G. H., Physica Scripta **T59**, 249 (1995).
27. Cody, R. B., Burnier, R. C. and Freiser, B. S., Anal. Chem. **54**, 96 (1982).
28. Becker, St. *et al.*, Rapid Commun. Mass Spectrom. **8**, 401 (1994).
29. Becker, St. *et al.*, Comp. Mat. Sci. **2**, 633 (1994).
30. Becker St. *et al.*, Z. Phys. **D30**, 341 (1994).
31. Dietrich, G. *et al.*, Ber. Bunsenges. Phys. Chem. **98**, 1608 (1994).
32. Elkind, J. L., Weiss, F. D., Alford, J. M., Laaksonen, R. T. and Smalley, R. E., J. Chem. Phys. **88**, 5215 (1988).
33. Ziegler, J. *et al.*, SASP 94, Symp. on Atomic and Surface Physics, Innsbruck, March 20–26, 1994, Maria Alm/Austria (Edited by T. D. Märk, R. Schrittwieser and D. Smith), p. 293–296.
34. Walther, C. *et al.*, Proc. 7th Int. Symp. Resonance Ionization Spec., Juli 3–8, 1994, Bernkastel-Kues, Germany, in print.
35. Weidele, H. *et al.*, Surface Rev. and Letters, in print.
36. Hvelplund, P., Physica Scripta **T59**, 244 (1995).